Oncogene (2004) 23, 6900–6913

www.nature.com/onc

The farnesyl transferase inhibitor R115777 (Zarnestra®) synergistically enhances growth inhibition and apoptosis induced on epidermoid cancer cells by Zoledronic acid (Zometa®) and Pamidronate

Michele Caraglia[1], Anna Maria D'Alessandro[1], Monica Marra[1], Gaia Giuberti[1], Giovanni Vitale[2], Caterina Viscomi[3], Annamaria Colao[2], Salvatore Del Prete[4], Pierosandro Tagliaferri[3], Pierfrancesco Tassone[3], Alfredo Budillon[5], Salvatore Venuta[3] and Alberto Abbruzzese*[,1]

[1]*Department of Biochemistry and Biophysics, II University of Naples, Via Costantinopoli no 16, 80138 Naples, Italy;* [2]*Department of Molecular and Clinical Endocrinology and Oncology, 'Federico II' University of Naples, Italy;* [3]*Department of Experimental and Clinical Medicine, University Magna Graecia of Catanzaro, Italy;* [4]*Oncology Department, Frattamaggiore, ASL NA3, Italy;* [5]*National Cancer Institute of Naples 'Fondazione G. Pascale', Italy*

Pamidronate (PAM) and zoledronic acid (ZOL) are aminobisphosphonates (BPs) able to affect the isoprenylation of intracellular small G proteins. We have investigated the antitumor activity of BPs and R115777 farnesyl transferase inhibitor (FTI) against epidermoid cancer cells. In human epidermoid head and neck KB and lung H1355 cancer cells, 48 h exposure to PAM and ZOL induced growth inhibition (IC_{50} 25 and 10 μM, respectively) and apoptosis and abolished the proliferative and antiapoptotic stimuli induced by epidermal growth factor (EGF). In these experimental conditions, ZOL induced apoptosis through the activation of caspase 3 and a clear fragmentation of PARP was also demonstrated. A strong decrease of basal ras activity and an antagonism on its stimulation by EGF was recorded in the tumor cells exposed to BPs. These effects were paralleled by impaired activation of the survival enzymes extracellular signal regulated kinase 1 and 2 (Erk-1/2) and Akt that were not restored by EGF. Conversely, farnesol induced a recovery of ras activity and antagonized the proapoptotic effects induced by BPs. The combined treatment with BPs and R115777 resulted in a strong synergism both in growth inhibition and apoptosis in KB and H1355 cells. The synergistic activity between the drugs allowed BPs to produce tumor cell growth inhibition and apoptosis at *in vivo* achievable concentrations (0.1 μmolar for both drugs). Moreover, the combination was highly effective in the inhibition of ras, Erk and Akt activity, while farnesol again antagonized these effects. In conclusion, the combination of BPs and FTI leads to enhanced antitumor activity at clinically achievable drug concentrations that resides in the inhibition of farnesylation-dependent survival pathways and warrants further studies for clinical translation.

*Correspondence: A Abbruzzese;
E-mail: Alberto.Abbruzzese@unina2.it and M Caraglia;
E-mail: Michele.Caraglia@unina2.it
Received 28 November 2003; revised 1 April 2004; accepted 14 April 2004; published online 2 August 2004

Oncogene (2004) **23,** 6900–6913. doi:10.1038/sj.onc.1207814
Published online 2 August 2004

Keywords: farnesyl transferase inhibitor; bisphosphonates; epidermoid cancer; apoptosis; ras; akt

Introduction

The enzymes of the mevalonate pathway play an important role in the modulation of several key cellular proteins, such as ras, rho, P × F and lamins A and B, because they induce the generation of isoprenoid intermediates that are required for the post-translational prenylation of these proteins (Schafer and Rine, 1992; Tamanoi *et al*., 2001). Prenylated proteins are critical intermediates of cell signalling and cytoskeletal organization (Schafer and Rine, 1992; Tamanoi *et al*., 2001); for instance, activated ras proteins trigger a cascade of phosphorylation events through sequential activation of the PI3 kinase/AKT pathway, which is critical for cell survival, and the Raf/Mek/Erk kinase pathway that is implicated both in cell proliferation and survival (Porter and Vaillancourt, 1998; Hilger *et al*., 2002). Ras proteins are among the most frequently mutated oncoproteins in human cancers (Haluska *et al*., 2002). Ras and other G proteins require localization to the inner surface of the cell membrane to function in signal transduction and cell transformation (Hancock *et al*., 1989; Aznar and Lacal, 2001). These G proteins are acylated and/or prenylated and these modifications act as membrane anchors for ras. Prenylation is catalysed by farnesyl transferase or geranylgeranyl transferase I that transfer to the protein substrate a farnesyl group or a geranylgeranyl group, respectively (DeSolms *et al*., 2003). The synthesis of both farnesyl and geranylgeranyl residues requires the activity of the farnesyl pirophosphate synthase, the upstream enzyme involved in the cholesterol synthesis chain (Schafer and Rine, 1992).

Therefore, prenylation process is mandatory for the correct membrane localization and function of several proteins involved in key cellular processes such as proliferation, differentiation, adhesion and tumorigenesis.

Bisphosphonates (BPs) such as pamidronate (PAM) and zoledronate (ZOL) are currently used for the treatment of bone metastases and were initially thought to act via an inhibition of formation of osteoclasts from immature precursor cells or direct inhibition of resorption via induction of apoptosis in mature osteoclasts (Hughes *et al*., 1995). Recently, evidence accumulated that BPs including PAM and ZOL are also potent inducers of apoptosis in several cancer cell types such as myeloma (Shipman *et al*., 1997; Aparicio *et al*., 1998; Tassone *et al*., 2000), breast (Senaratne *et al*., 2000), prostate cancer (Lee *et al*., 2001) and pancreatic cancer (Tassone *et al*., 2003), as well as in macrophage (Rogers *et al*., 1996) and intestinal epithelial cell lines (Twiss *et al*., 1999). These data indicate that the beneficial effect of BPs on metastatic bone disease may result also from a direct anticancer activity that may affect a broad range of tumors. In addition, nitrogen-containing BPs were shown to inhibit the farnesyl diphosphate synthase probably by mimicking the diphosphate moiety (Van Beek *et al*., 1999a, b). Therefore, they are inhibitors of the synthesis also of higher isoprenoids like geranylgeranyl diphosphate.

A series of specific and potent inhibitors of farnesyl transferase (FTI) has been synthesized up –to date . Generally, FTIs are analogues of the COOH CAAX tetrapeptides of ras that specifically interact with the FT before transferring the farnesyl residue (Sebti and Hamilton, 2000). It was generally thought that they would predominantly inhibit the growth of ras-dependent tumors. However, studies have suggested that ras may not be the sole or even the main target of these compounds, and novel intriguing mechanisms have been hypothesized on the bases of experimental results (Lebowitz *et al*., 1997; Lebowitz and Prendergast, 1998; Selleri *et al*., 2003). Moreover, it was demonstrated that FTIs can block the activity of a number of downstream targets of ras that may be involved in cell survival, such as Erk and Akt (Smalley and Eisen, 2002). FTIs inhibit the farnesylation of ras and of other small G proteins involved in cell proliferation and survival, but alternative mechanisms of prenylation, such as the geranylgeranylation, also exist (Sebti and Hamilton, 2000). Moreover, an important recent finding is that FTI inhibition of K-Ras-transformed cells may be independent of K-Ras inhibition itself (Fiordalisi *et al*., 2003).

All these events together with the occurrence of escape mechanisms could be the cause of the substantial clinical failure of FTIs when used alone against human solid tumors. The combination of BPs and FTIs appears, therefore, a potential approach for increasing the antitumor activity of both compounds.

In the present paper, we have investigated growth inhibition and apoptosis induced by PAM and ZOL in human epidermoid cancer cells. We have characterized the molecular targets of BPs and the interaction with the EGF-dependent signalling and we have specifically investigated the effect induced by the BPs on the Akt and Erk survival pathways. We have studied the pharmacological interactions between BPs and the FTI R115777 in order both to reduce BPs concentration required for the antitumor activity and to overcome potential mechanisms of cell resistance to R115777. We have actually studied the effects of the combination on growth inhibition and apoptosis of human epidermoid cancer cells and we have again characterized the molecular targets involved in such effects.

The main goal of our investigation has been the study of a molecularly based rational model of antitumor treatment based on BPs and FTI combination.

Results

PAM and ZOL induce growth inhibition and apoptosis in human epidermoid cancer cells that are not antagonized by EGF

We have evaluated the effects of BPs and EGF on growth inhibition of both human head and neck cancer KB and lung H1355 cell lines.

PAM and ZOL induced a time- and dose-dependent growth inhibition in both cell lines (Figure 1a and b). The 50% growth inhibition was reached at PAM concentration of 25 μM and ZOL concentration of 10 μM after 48 h of treatment in both cell lines (Figure 1a and b). On the other hand, 72 h 10 nM EGF alone caused proliferation and an about 35% increase of the cell number in the S phase fraction of the cell cycle on both cell lines (Figure 1c and data not shown). The concomitant exposure of KB and H1355 cells to 10 nM EGF for 48 and 72 h did not, however, antagonize the growth inhibition induced by the BPs (Figure 1c).

In these experimental conditions, apoptosis was detected in both cell lines. In fact, endonucleosomal DNA fragmentation and an increase of apoptosis was determined by 48 h 25 μM PAM and 10 μM ZOL on about 50% of KB cell population as assessed with gel ladder and FACS analysis after PI labelling, respectively (Figure 2a, d and f). Also in this case, the concomitant addition of 10 nM EGF for 48 h was not able to antagonize the effects induced by PAM and ZOL on the epidermoid cancer cells (Figure 2a, e and g). Similar effects were produced also by the addition of 25 μM PAM and 10 μM ZOL to H1355 cells for 48 h (Figure 2h). Also in the latter case, EGF was not able to antagonize the effect induced by BPs (Figure 2h). These data indicate that BPs exert direct growth inhibitory and proapoptotic effects on human epidermoid cancer cells and also desensitizes tumor cells to the growth promoting and antiapoptotic effects of EGF.

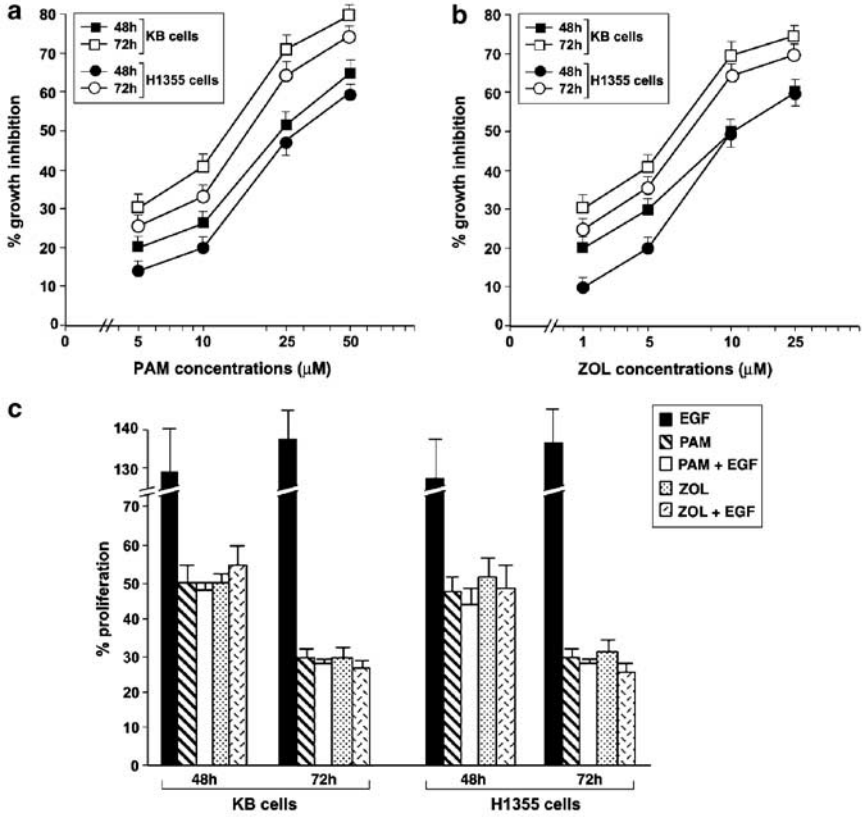

Figure 1 PAM induces growth inhibition that is not antagonized by EGF in human epidermoid cancer cells. KB and H1355 cells were seeded and treated with PAM (**a**) or ZOL (**b**) as described in Materials and methods. (**a**, **b**) % growth inhibition induced by different concentrations of PAM (**a**) and ZOL (**b**) in human KB and H1355 cells evaluated with hemocytometric cell count. The 48 h (■) and 72 h (□) PAM- or ZOL-treated KB cells and 48 h (•) and 72 h (○) PAM- or ZOL-treated H1355 cells. Each point is the mean of at least four different replicate experiments. Bars, s.e.'s. (**c**) KB and H1355 cells were seeded and treated with 25 μM PAM or 10 μM ZOL and/or 10 nM EGF for 48 and 72 h as described in 'Materials and methods'. The effects on proliferation are expressed as % of cell growth as compared to untreated cells. EGF: 10 nM EGF-treated cells; PAM: 25 μM PAM-treated cells; ZOL: 10 μM ZOL-treated cells; PAM + EGF: 10 nM EGF and 25 μM PAM-treated cells; ZOL + EGF:10 nM EGF and 10 μM ZOL-treated cells. Each point is the mean of at least four different replicate experiments. Bars, s.e.'s

Caspase cascade is involved in the apoptosis induced by ZOL in KB cells

We have also investigated on the role of caspase activity in the apoptosis induced by ZOL. We have treated KB cells with different and specific inhibitors of caspases added to the medium 1 h before the treatment with ZOL for 48 h and, then, apoptosis was evaluated at FACS analysis. We have found that the pancaspase inhibitor VADfmk and caspase 3 inhibitor DEVDfmk completely antagonized the apoptosis induced by ZOL (Figure 3b, c and e). In fact, ZOL induced 49% apoptosis, while the pancaspase and caspase 3 inhibition restored apoptosis to control values (9%) (Figure 3b, c and e). On the other hand, the inhibition of caspases 6, 8 and 1 antagonized only in part the apoptosis induced by ZOL. In fact, in caspase 6 inhibitor-treated cells, ZOL induced an about 26% apoptosis (Figure 3d). Moreover, in caspase 8 inhibitor-treated and caspase 1 inhibitor-treated cells, apoptosis was found in about 27 and 30% of cells, respectively (Figure 3f and g, respectively). We also found that exposure of KB cells to 10 μM ZOL for 48 h increased PARP cleavage, a key enzyme in the apoptotic cascade, as demonstrated by Western blot analysis, which showed the appearance of an 89 kDa cleavage product in treated cells (Figure 3h). Therefore, caspase cascade is involved in the apoptosis induced by ZOL in epidermoid cancer cells and caspase 3 seems to be essential for the occurrence of programmed cell death in these experimental conditions.

BPs effects on tumor cell apoptosis and ras signalling are caused by inhibition of protein isoprenylation

Since BPs affect the isoprenyl synthesis in tumor cells and an important mechanism of activation of ras (one of the major downstream enzymes of the EGF-dependent pathway) is its isoprenylation, we have evaluated the effects of BPs on ras activity. Notably, in this and all the following experiments, EGF was added for short-term exposures in order to evaluate the responsiveness of each signaling component to its physiological ligand. We have found that 48 h 25 μM PAM or 10 μM ZOL did not induce changes of the ras expression levels but caused an about 60% decrease of ras activity as

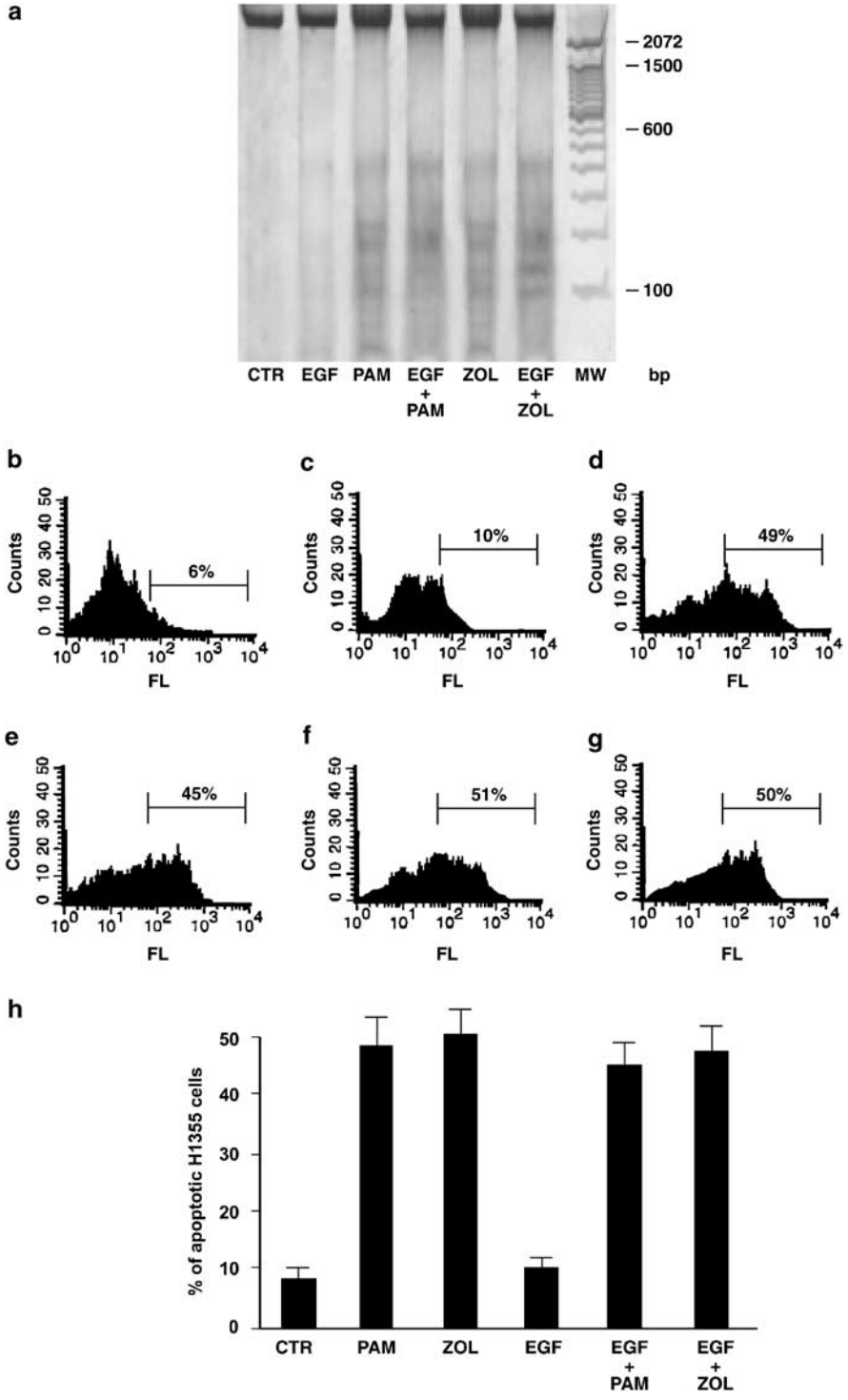

Figure 2 Apoptotic effects of PAM on human epidermoid KB cells. (**a**) The internucleosomic DNA fragmentation was assessed as described in 'Materials and methods'. The exposure of KB cells to PAM (25 μM) or to ZOL (10 μM) for 48 h induced apoptosis that was not antagonized by the concomitant addition of 10 nM EGF. The experiments were performed at least three times and the results were always similar. CTR, untreated; EGF, 48 h 10 nM EGF; PAM, 48 h 25 μM PAM; EGF + PAM, 48 h 10 nM EGF and 25 μM PAM; ZOL, 48 h 10 μM ZOL; EGF + ZOL, 48 h 10 nM EGF and 10 μM ZOL; MW, molecular weights. (**b-g**) FACS analysis after PI labelling of KB cells treated with 25 μM PAM and/or 10 nM EGF for 48 h. (**b**) Control cells; (**c**) 48 h 10 nM EGF-treated cells; (**d**) 48 h 25 μM PAM-treated cells; (**e**) 48 h 25 μM PAM- and 10 nM EGF-treated cells; (**f**) 48 h 10 μM ZOL-treated cells; (**g**) 48 h 10 nM EGF and 10 μM ZOL-treated cells. The experiments were performed at least three times and the results were always similar. Bars, % of apoptotic cells. (**h**) FACS analysis after PI labelling of H1355 cells treated with 25 mM PAM or 10 μM ZOL and/or 10 nM EGF for 48 h. Percentage of apoptotic cells is expressed as columns. The experiments were performed at least three times and the results were always similar. CTR, untreated; PAM, 48 h 25 μM PAM; ZOL, 48 h 10 μM ZOL; EGF, 10 min 10 nM EGF; EGF + PAM, 10 min 10 nM EGF and 48 h 25 μM PAM; EGF + ZOL, 48 h 10 nM EGF and 10 μM ZOL. Bars, s.e.'s

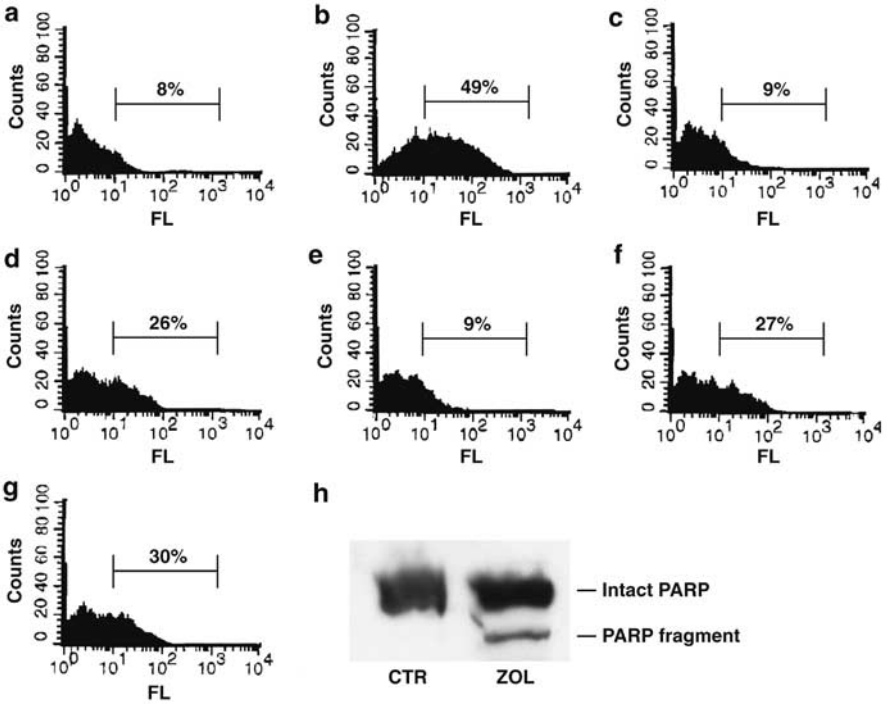

Figure 3 Involvement of caspase cascade in the apoptosis induced by ZOL in human epidermoid cancer cells. (**a**–**g**) We have treated KB cells with different and specific inhibitors of caspases added to the medium 1 h before the treatment with ZOL for 48 h and, then, apoptosis was evaluated at FACS analysis as described in 'Materials and methods'. (**a**) Control cells; (**b**) 48 h 10 μM ZOL-treated cells; (**c**) 48 h 10 μM ZOL and 10 μM VAD fmk-treated cells; (**d**) 48 h 10 μM ZOL and 10 μM VEID fmk-treated cells; (**e**) 48 h 10 μM ZOL and 10 μM DEVD fmk-treated cells; (**f**) 48 h 10 μM ZOL and 10 μM IETD fmk-treated cells; (**g**) 48 h 10 μM ZOL and 10 μM YVAD fmk-treated cells. The experiments were performed at least three times and the results were always similar. Bars, % of apoptotic cells. (**h**) Detection of PARP in KB cells after ZOL treatment. Western blotting analysis was performed on protein extracts from solubilized whole-cell pellets from KB cell lines after 48 h exposure to ZOL (10 μM), demonstrating abundant cleaved species of PARP in lysates for drug-exposed cells. The experiments were performed at least three times and the results were always similar

evaluated by Western blotting analysis and affinity precipitation with the minimal binding domain of raf-1, respectively (Figure 4a–c). As expected, EGF alone induced an increase in the activity of ras in the absence of changes in its expression (Figure 4a–c), but the concomitant exposure to 10 nM EGF was not able to antagonize the effects of BPs on both ras expression and activity (Figure 4a–c), suggesting that the lack of activation of ras by the EGF-R was the cause of signalling inhibition produced by BPs. In order to investigate on the role of protein prenylation on ras signalling and apoptosis induced by BPs, we have exposed PAM- and ZOL-treated KB cells to farnesol. We have found that farnesol was indeed able to antagonize the proapoptotic effects of BPs (Figure 4f and h) as evaluated by FACS analysis. In fact, in KB cells treated for 48 h with 25 μM PAM or 10 μM ZOL plus 1 μM farnesol, only about 10% of cell population was apoptotic (Figure 4f and h). We have found that at the same experimental conditions, 25 μM PAM and 10 μM ZOL decreased ras signalling activity, which was, however, almost completely restored by the concomitant treatment with farnesol as evaluated by Western blotting analysis and an affinity precipitation assay (Figure 4i and j, respectively). We have also performed the concomitant treatment of tumor cells with BPs and EGF for 48 h and again EGF was not able to antagonize the effects of BPs on ras expression and activity (data not shown). All together, these findings indicate that the effects of BPs on apoptosis and ras-signalling in human epidermoid tumor cells rely on the inhibition of isoprenylation of critical transducing proteins.

Effects of BPs on terminal survival Erk and Akt enzymes

We have evaluated the effects of PAM and ZOL on the terminal enzymes of the survival MAPK pathway, Erk-1 and Erk-2. We have found that both 48 h 25 μM PAM and 10 μM ZOL induced an about threefold decrease of Erk-1 and 2 activity as evaluated with a Western blotting assay using a Mab raised against the phosphorylated/activated isoforms of the two enzymes (Figure 5b). On the other hand, at the same experimental conditions, BPs did not induce substantial changes of Erk-1/2 expression, thus suggesting a direct effect on enzyme activation induced by the upstream regulators more than that on enzyme expression/content (Figure 5a). Tumor cell exposure for 10 min to 10 nM EGF alone induced a twofold increase of enzyme activity in epidermoid cells (Figure 5b), but again it was not able to antagonize the inhibitory effects of PAM on Erk activity (Figure 5a and b). Thereafter, we have evaluated the effects of BPs on another important survival pathway regulated

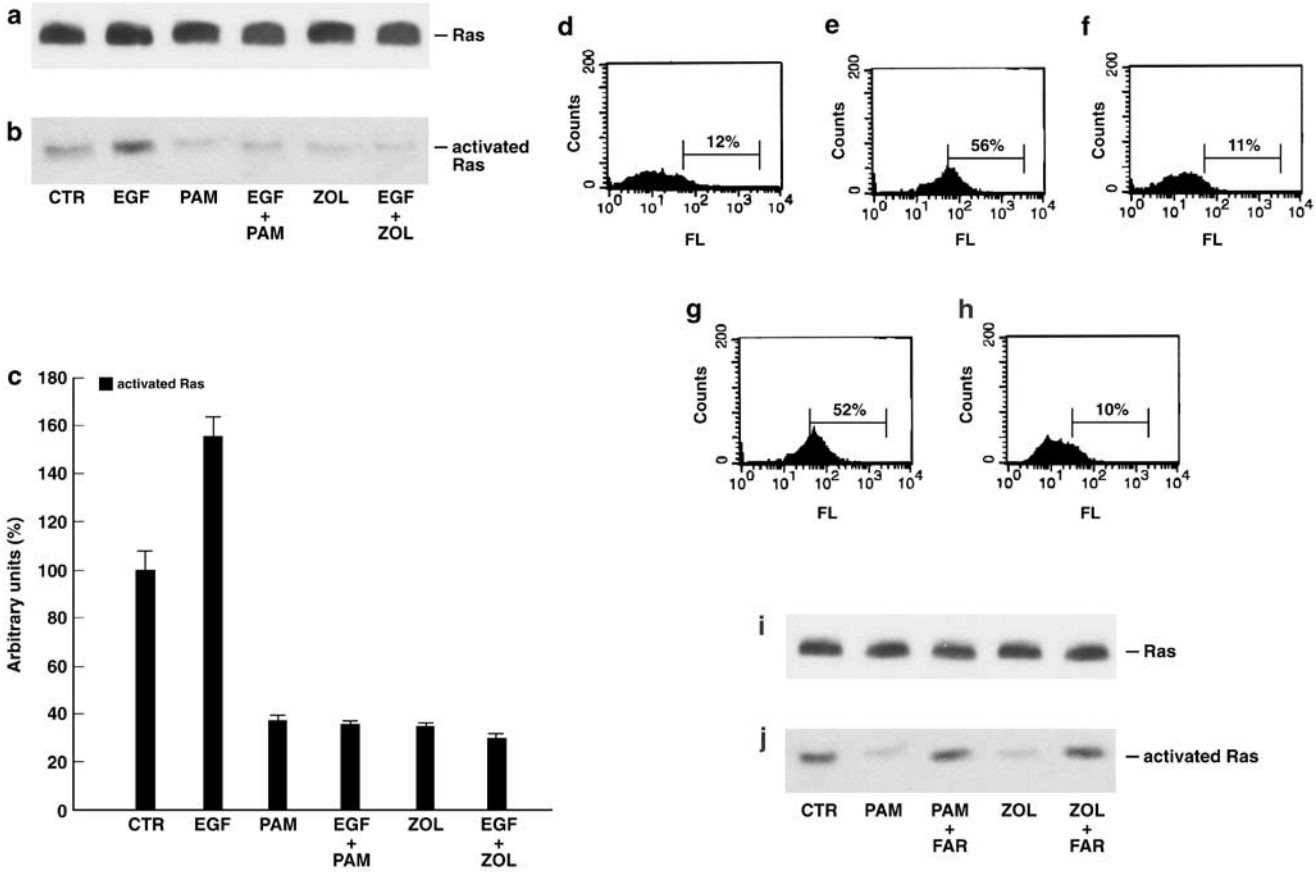

Figure 4 Effects of PAM and EGF on ras expression and activity. (**a**) Western blot assay for the expression of the total ras protein. (**b**) Affinity precipitation of ras performed with the minimal binding domain of raf-1 conjugated with agarose for the evaluation of ras activity as described in 'Materials and methods'. (**c**) Scan of the bands associated with ras expression and activity was performed with a dedicated software and the ratio between activated ras and total ras was calculated and expressed as % of control (mean of three different experiments). Bars, s.e.'s. CTR, untreated; EGF, 10 min 10 nM EGF; PAM, 48 h 25 μM PAM; EGF + PAM, 10 min 10 nM EGF and 48 h 25 μM PAM; ZOL, 48 h 10 μM ZOL; EGF + ZOL, 48 h 10 nM EGF and 10 μM ZOL. The experiments were performed at least three different times and the results were always similar. (**d**–**h**) FACS analysis after PI labelling of KB cells treated with 25 μM PAM and/or 1 μM farnesol for 48 h. (**d**) Control KB cells; (**e**) 48 h 25 μM PAM-treated KB cells; (**f**) 48 h 25 μM PAM and 1 μM farnesol-treated KB cells; (**g**) 48 h 10 μM ZOL-treated KB cells; (**h**) 48 h 10 μM ZOL and 1 μM farnesol-treated KB cells. The experiments were performed at least three different times and the results were always similar. Bars, % of apoptotic cells. Total ras expression (**i**) and activity (**j**) of BPs and/or farnesol-treated KB cells evaluated as described above. CTR, untreated; PAM, 48 h 25 μM PAM; PAM + FAR, 48 h 25 μM PAM and 1 μM farnesol; ZOL, 48 h 10 μM ZOL; ZOL + FAR, 48 h 25 μM ZOL and 1 μM farnesol. The experiments were performed at least three different times and the results were always similar

by EGF and ras, the Akt/PKB signalling. In details, we have studied both Akt expression and activity with Western blotting and in gel kinase assay, respectively. We have found that both BPs induced an about 2.5-fold decrease of Akt activity without apparent modifications of its expression (Figure 5d and c, respectively). Also, in this case, 10 min 10 nM EGF did not restore Akt activity.

All these data indicate that the effects of BPs on growth inhibition and apoptosis in epidermoid cancer cells KB are paralleled by the disruption of two different survival pathways, both of them important targets of ras function.

BPs and the FTI R115777 have a synergistic effect on KB cell growth inhibition

Since the concentrations of BPs that are capable to produce growth inhibitory and proapoptotic effects on tumor cells *in vitro* are difficult to be reached *in vivo*, we have investigated on a novel experimental approach to increase the translational potential of our findings. Specifically, we have combined another isoprenylation inhibitor (the FTI R115777) with BPs. Thereafter, we have evaluated the growth inhibition induced by different concentrations of PAM or ZOL in combination with R115777 at 48 h on KB and H1355 cells. We have performed these experiments with MTT assay and the resulting data were elaborated with the dedicated software Calcusyn (by Chou and Talalay, see also 'Materials and methods'). With this mathematical model, synergistic conditions occur when the combination index (CI) is below 1.0. When CI is less than 0.5, the combination is highly synergistic. We have found that the combination of PAM and R115777 was highly synergistic when the two drugs were used at equitoxic concentrations while overwhelming concentrations of

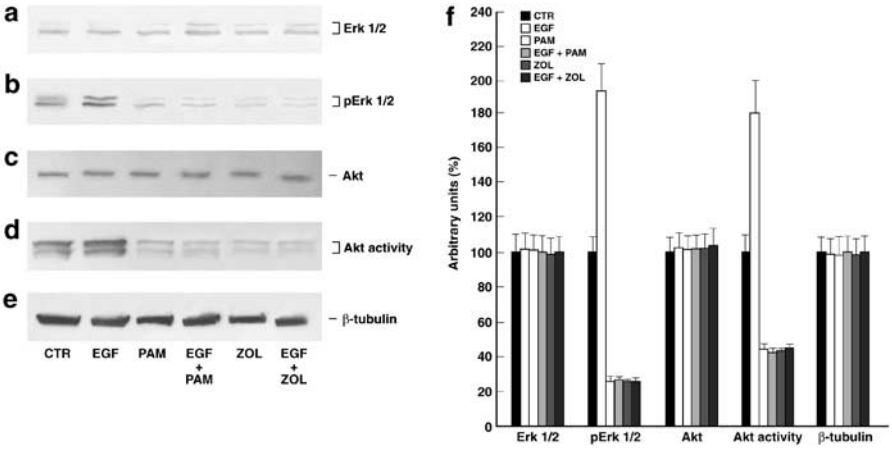

Figure 5 BPs decrease Erk-1/2 and Akt activity in human epidermoid cancer cells. KB cells have been cultured for 48 h in the absence or presence of 25 μM PAM or 10 μM ZOL and/or 10 nM EGF. Then the cells were processed for the determination of the expression (**a**) and phosphorylation (**b**) of erk-1 and 2 evaluated after blotting with an anti-MAPK- and an anti-pMAPK-specific Mab, respectively, as described in 'Materials and methods'. In the same experimental conditions, the expression (**c**) and activity (**d**) of Akt was also analysed with a Western blotting and an in-gel kinase assay, respectively, as described in 'Materials and methods'. (**e**) Expression of the house-keeping protein β-tubulin, used as loading control. The experiments were performed at least three different times and the results were always similar. CTR, untreated; EGF, 10 min 10 nM EGF; PAM, 48 h 25 μM PAM; EGF + PAM, 10 min 10 nM EGF and 48 h 25 μM PAM; ZOL, 48 h 10 μM ZOL; EGF + ZOL, 48 h 10 nM EGF and 10 μM ZOL. (**f**) Scan of the bands associated with Erk 1/2 and Akt expression and activity was performed with a dedicated software and the intensities of the bands were expressed as arbitrary units (%, mean of three different experiments). Bars, s.e.'s

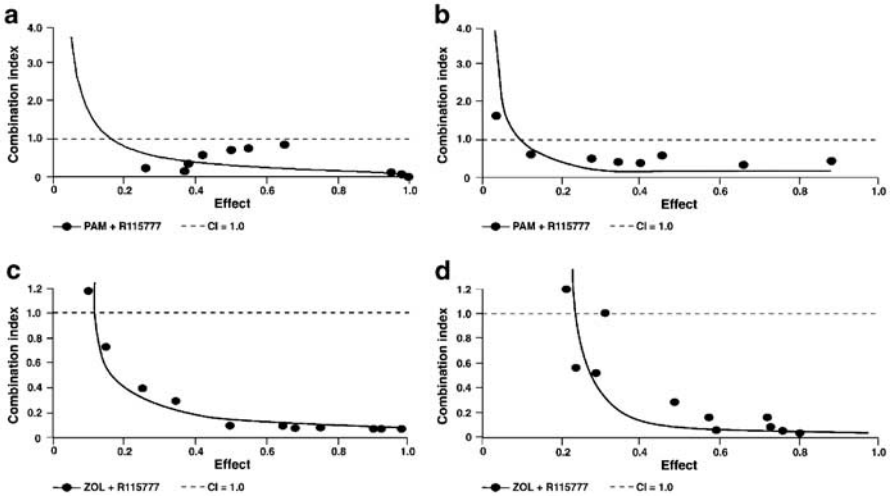

Figure 6 PAM and the FTI R115777 have a synergistic effect on KB cell growth inhibition. We have evaluated the growth inhibition induced by different concentrations of PAM or ZOL and R115777 at 48 h on KB cells. We have performed these experiments with MTT assay and the resulting data were elaborated with the dedicated software Calcusyn (by Chou and Talalay) as described in 'Materials and methods'. In the figure, it is shown the isobologram analysis of the effects of PAM and R115777 combinations, used at equitoxic concentrations, on growth inhibition of KB (**a**) and H1355 (**b**) cells and of the effects of ZOL and R115777 combinations, used at overwhelming concentrations of ZOL, on growth inhibition of KB (**c**) and H1355 (**d**) cells. CI, combination index. Each point is the mean of at least four different replicate experiments

either PAM or FTI were not (Figure 6a and b and data not shown). In synergistic drug combination, the CI_{50}s (the combination index calculated for 50% cell survival by isobologram analysis) were 0.24 and 0.26 for KB and H1355 cells, respectively (Table 1). Therefore, the combined use of the two agents was highly synergistic on the growth inhibition of both cell lines. Dose reduction $index_{50}$ (DRI_{50}) represents the magnitude of dose reduction obtained for the 50% growth inhibitory effect in combination setting as compared to each drug alone. In our experimental conditions, the DRI_{50} of PAM and FTI were equal to 260 and 280 in KB and 200 and 300 in H1355 cells, respectively, when the two drugs were used at equitoxic concentrations (Table 1). Also, ZOL and R11577 combination resulted synergistic on the growth inhibition of both KB and H1355 cells. In fact, we have found that the combination of ZOL and R115777 was highly synergistic when overwhelming

Table 1 Combination index[a] (CI) and dose reduction index[b] (DRI) values for PAM and R11577 combination

Cell lines	*PAM* ED_{50} (μm)	*R11577* ED_{50} (μm)	*Combination ratio (PAM/R11577)*	CI_{50}	DRI_{50}	*Interpretation*
					PAM:260	Strong synergism
KB	0.1	0.1	1 : 1	0.24	R11577 : 280	Strong synergism
					PAM:260	Strong synergism
H1355	0.2	0.2	1 : 1	0.26	R11577 : 280	Strong synergism
Cell lines	*ZOL* ED_{50} (μm)	*R11577* ED_{50} (μm)	*Combination ratio (ZOL/R11577)*	CI_{50}	DRI_{50}	*Interpretation*
KB	0.25	0.08	3 : 1	0.1	ZOL:33	Very strong synergism
					R11577 : 220	Very strong synergism
H1355	0.25	0.08	3 : 1	0.1	ZOL:33	Strong synergism
					R11577 : 110	Strong synergism

[a]CI_{50} were calculated for 50% cell survival (ED_{50}) by isobologram analyses performed with CalcuSyn software. [b]DRI represents the order of magnitude (fold) of dose reduction obtained for ED_{50} effect in combination setting as compared to each drug alone

concentrations of ZOL were used on both KB and H1355 cells (Figure 6c and d, respectively). In these conditions, the CI_{50}s were 0.1 and 0.25 for KB and H1355 cells, respectively (Table 1). The DRI_{50} of both ZOL and FTI were equal to 30 and 220 on KB and 10 and 110 on H1355 cells, respectively (Table 1). These results demonstrate that a strong or a very strong synergism can be recorded on cell proliferation when the two drugs are used in combination. Effective concentrations in the combinatory experiments are possible to be reached *in vivo*.

BPs and the FTI R115777 have a synergistic effect on apoptosis in KB cells

We have selected two combinations of R115777 and PAM that were highly synergistic at Calcusyn elaboration and we have evaluated the apoptotic effects of such combination with FACS analysis after labelling for annexin V and at fluorescence microscopy with double PI and annexin V labelling. We have found that the treatment with 0.07 μM R115777 and PAM alone for 48 h had no effect on apoptosis of KB and H1355 cells (Figure 7b, c and f, respectively). In fact, only about 7.5–10% of cell population was apoptotic (similarly to control cells) when KB and H1355 cells were treated with the two drugs alone as demonstrated with FACS analysis and double fluorescence technique (Figure 7a–c and f and related insets). However, when the cells were treated with the two drugs in combination for 48 h, about 40% of apoptosis was found in both cell lines (Figure 7d and f, respectively). Moreover, a great increase of red or green fluorescent cells was detected in the combined treatment as compared to the single treatment points (Figure 7). In the same experimental conditions, farnesol antagonized the effects of R115777 and PAM combination on the apoptotic onset (Figure 7e and f). In fact, the apoptosis induced by the combination was completely antagonized by the concomitant addition of 1 μM farnesol since, at these experimental conditions, only 9% of apoptosis was detected on both KB and H1355 cells (Figure 7e and f, respectively). Analogous results were obtained when KB and H1355 cells were treated with 0.6 μM ZOL and 0.07 μM R115777 combination since the two drugs alone caused an about 10% apoptosis and the combination an about 40–50% of apoptosis on both cell lines (Figure 7g). Also in this case, farnesol completely inhibited the synergistic effects of the two drugs (Figure 7g). Notably, farnesol alone did not cause significant changes in apoptotic index on both these cell lines (data not shown). These data suggest that the synergism on cell growth inhibition induced by BPs and R115777 could be mediated by the induction of apoptosis in human epidermoid cancer cells through the inhibition of farnesylation.

Effects of BP PAM and FTI R115777 combination on survival signalling

We have evaluated the effects of the PAM/R115777 synergistic combination on signal transduction pathways in cancer cells. In details, we have evaluated the effects on ras expression and activity and we have performed the laser scanner of the bands associated to total and activated ras and we have calculated the ras activation ratio (rasAR) given by the ratio between the intensities of the bands associated with ras activity and expression, respectively. We have found that PAM and R115777 alone induced a 40 and 30% reduction of rasAR, respectively (Figure 8a–c). However, when cells were treated with the two agents together, a 80% decrease of rasAR was recorded (Figure 8a–c). Thereafter, we have evaluated the effects of the combination on two downstream survival signalling targets: Erk and Akt. PAM and R115777 alone or in combination did not induce any change of Erk-1/2 expression as evaluated with Western blot analysis (Figure 8d). PAM and R115777 alone induced both an about 35% decrease of Erk activity, while the combination caused an about 85% decrease of Erk activity (Figure 8e and i). PAM and R115777 alone or in combination again did

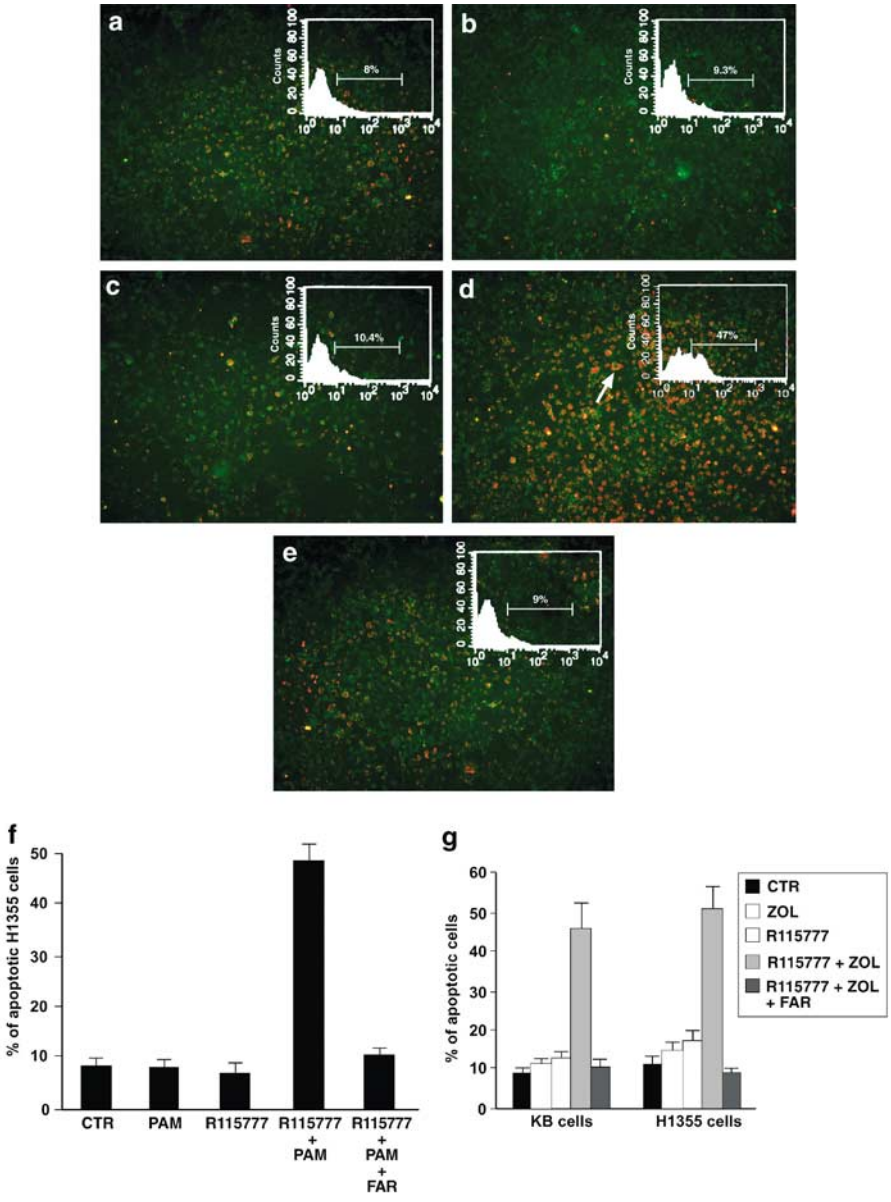

Figure 7 BPs and the FTI R115777 combination have a synergistic effect on apoptosis that was antagonized by farnesol supplementation in KB and H1355 cells. We have selected a combination of R11577 and PAM that was highly synergistic at Calcusyn elaboration and gave an about 40% growth inhibition. We have evaluated the apoptotic effects of this combination and the antagonistic activity of farnesol on KB (**a**–**e**) and H1355 (**f**) cells at fluorescence microscopy after PI and anti-annexin V antibody (photos) and at FACS analysis after anti-annexin V antibody labelling (insets). (**a**) Control cells; (**b**) 48 h 0.07 μM R115777; (**c**) 48 h PAM 0.07 μM; (**d**) 48 h 0.07 μM R115777 and PAM 0.07 μM; (**e**) 48 h 0.07 μM PAM and 0.07 μM R115777 and 1 μM farnesol. Red and green fluorescent cells were apoptotic. The bars in the insets show the percentage of apoptotic cells. Arrows show apoptotic cells. (**f**) The same experiment was performed on H1355 cells, and apoptosis was evaluated at FACS analysis after anti-annexin V antibody labelling. Apoptotic cells are shown as columns. CTR, control cells; PAM, 48 h 0.07 μM PAM; R115777, 48 h 0.07 μM R115777; R115777 + PAM 48 h, 0.07 μM R115777 and 0.07 μM PAM; R115777 + PAM + FAR, 48 h 0.07 μM PAM and 0.07 μM R115777 and 1 μM farnesol. Bars, s.e.'s. (**g**) The same experiment was performed on KB and H1355 cells using a combination of R115777 and ZOL that was synergistic on cell growth inhibition at CalcuSyn evaluation. Apoptosis was evaluated at FACS analysis after anti-annexin V antibody labelling and are shown as columns. CTR, control cells; ZOL, 48 h 0.6 μM ZOL; R115777, 48 h 0.07 μM R115777; R115777 + ZOL 48 h, 0.07 μM R115777 and 0.6 μM ZOL; R115777 + ZOL + FAR, 48 h 0.6 μM ZOL and 0.07 μM R115777 and 1 μM farnesol. The experiments were performed at least three different times and the results were always similar. Bars, s.e.'s

not change Akt expression (Figure 8f and i). However, PAM and R115777 alone induced an about 35 and 20% reduction of Akt activity while the combination caused a 80% decrease of its activity (Figure 8g and i). Therefore, concomitant treatment always induced a more than additive decrease of ras, Erk and Akt activities and this effect appears to correlate with the growth inhibition and apoptotic induction experiments. We also found that when 1 μM farnesol was added to KB cells treated with the combination, all the effects on

the antiapoptotic ras-dependent pathways were antagonized providing further support to the concept that inhibition of prenylation played an essential role in the antitumor effects of the compound combinations (Figure 7a–i). These data also suggested that when KB cells were treated with low concentrations of compounds, the signalling pathways were slightly affected likely due to the instauration of escape mechanisms based on alternative isoprenylation pathways (R115777) or not efficient prenylation inhibition induced by PAM.

Discussion

BPs are commonly used in malignant and benign diseases involving excessive bone resorption such as osteolytic bone metastases and osteoporosis. BPs, particularly PAM and ZOL, have demostrated beneficial effects on skeletal metastases (Coleman *et al*., 1988; Morton *et al*., 1988; Fleisch, 1991; Averbuch, 1993; Lipton *et al*., 1994; Cascinu *et al*., 1998; Ali *et al*., 2001; Vitale *et al*., 2001). These drugs act through the induction of osteoclast apoptosis, probably due to the inhibition of the isoprenylation of proteins required for the osteoclast survival (Benford *et al*., 1999; Van Beek *et al*., 1999a, b; Luckman *et al*., 1998). However, a direct antitumor effect of BPs has been demonstrated in several cancer cell types such as multiple myeloma (Shipman *et al*., 1997; Aparicio *et al*., 1998; Tassone *et al*., 2000), breast (Senaratne *et al*., 2000), prostate (Lee *et al*., 2001) and pancreatic cancer cells (Tassone *et al*., 2003). It has been demonstrated that nitrogen-containing BPs directly induced apoptosis in tumor cells by affecting enzymes of the cholesterol metabolic pathway involved in the prenylation of small GTP-binding proteins (Luckman *et al*., 1998). In addition, BPs have marked antiangiogenetic properties (Wood *et al*., 2002) and inhibit the proteolytic activity of matrix metalloproteinases, mandatory for cell migration and digestion of the basement membrane (Boissier *et al*., 2000).

R115777 is a potent and selective nonpeptidomimetic competitive FTI (End, 1999; End *et al*., 2001) with antitumor activity as demonstrated by several *in vitro* and *in vivo* studies. Although R115777 has been initially developed as ras inhibitor, it is now clear that antitumor activity of R115777 may be correlated to the effects on a variety of proteins that require post-translational modification by prenylation (Kelland *et al*., 2001).

It is well known that EGF is an antiapoptotic factor and the EGF-induced ras activation has been correlated to these effects (Tilly *et al*., 1992; Peng *et al*., 1998; Stoll *et al*., 1998; Sibilia *et al*., 2000). In fact, EGF acts through the binding to its specific receptor, EGF-R, a

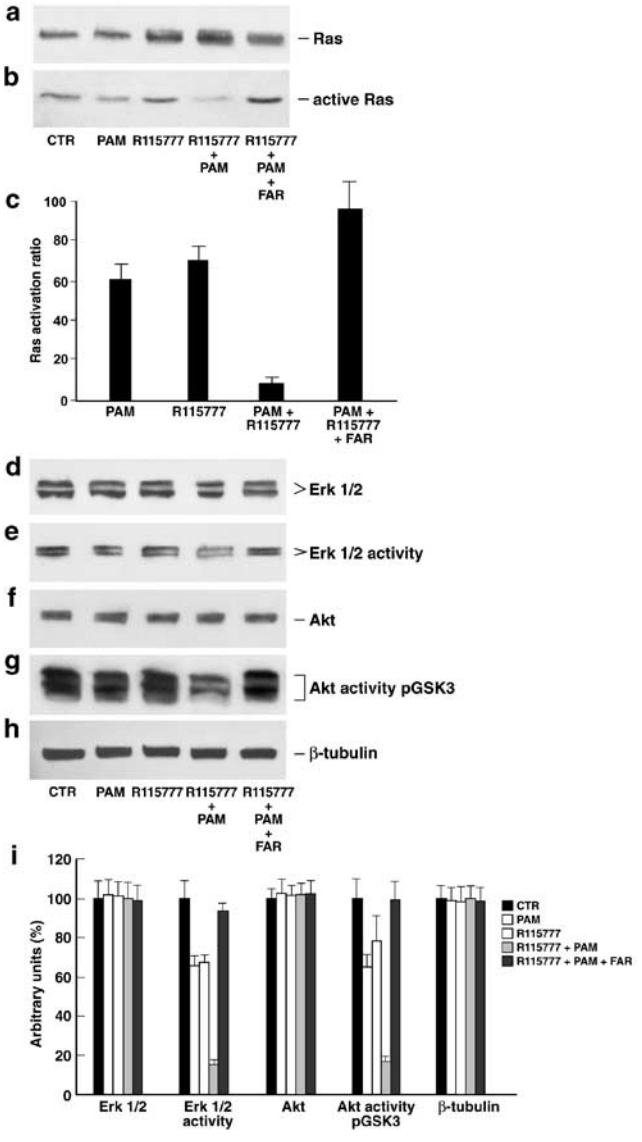

Figure 8 PAM and the FTI R115777 effects on ras-dependent survival pathways in KB cells. (**a**) Western blot assay for the expression of the total ras protein. (**b**) Affinity precipitation of ras performed with the minimal binding domain of raf-1 conjugated with agarose for the evaluation of ras activity as described in 'Materials and methods'. (**c**) Representation of the ras activation ratio expressed as the ratio between the relative intensities of the bands associated with activated ras versus the bands associated with total ras $\times 100$. The evaluation was performed with the dedicated software after laser scanner and computer-assisted acquisition of the bands. The intensity of each band was calculated in relative intensity as compared to that one of the untreated cells. Bars, s.e.'s. Determination of the expression (**d**) and phosphorylation (**e**) of erk-1 and 2 evaluated after blotting with an anti-MAPK and an anti-pMAPK specific Mab, respectively, as described in 'Materials and methods'. Evaluation of the expression (**f**) and activity (**g**) of Akt analysed with a Western blotting and an in-gel kinase assay, respectively, as described in Materials and methods. (**h**) Expression of the house-keeping protein β-tubulin, used as loading control. CTR, untreated; PAM, 48 h 0.07 μM PAM; R115777, 48 h 0.07 μM R115777; R115777 + PAM, 48 h 0.07 μM PAM + 0.07 μM R115777; R115777 + PAM + FAR, 48 h 0.07 μM PAM and 0.07 μM R115777 and 1 μM farnesol. All the experiments were performed at least three different times and the results were always similar. (**i**) Scan of the bands associated with Erk 1/2 and Akt expression and activity was performed with a dedicated software and the intensities of the bands were expressed as arbitrary units (%, mean of three different experiments). Bars, s.e.'s

transmemembrane protein with a cytoplasmic tyrosine kinase domain (Garrington and Johnson, 1999; Widmann *et al*., 1999). The phosphorylation of the intracytoplasmic tail allows the interaction of EGF-R with cytoplasmic factors that can induce ras activation when ras is isoprenylated and, therefore, linked to the inner side of the cell membrane. In fact, the latter event allows its interaction for colocalization with EGF-R-associated nucleotide exchange factors that favor GTP : GDP exchange and the subsequent ras activation. The stimulation of ras induces the triggering of several antiapoptotic and proliferative pathways and causes dramatic changes in cell shape. One of the most important survival pathways activated by ras is the mitogen-activated protein kinase (MAPK) cascade composed by three intracellular protein kinases (MKKK, MKK and MAPK), which are sequentially activated by phosphorylation (Widmann *et al*., 1999; Garrington and Johnson, 1999).The cascade finally induces the stimulation of the MAPKs, Erk 1 and 2 (Widmann *et al*., 1999; Garrington and Johnson, 1999)that mediate strong antiapoptotic effects (Aikawa *et al*., 1997; Yan and Greene, 1998).

A second important antiapoptotic pathway regulated by EGF and ras is the signalling via Akt/PKB (Zhou *et al*., 2000; von Gise *et al*., 2001). In fact, it has been demonstrated that Akt can be activated concomitantly or independently from Ras->ERK-1/2 signalling by growth factors (Kuo *et al*., 2001; Liu *et al*., 2001; Mitsui *et al*., 2001). Additionally, it has been reported that PC12 pheocromocytoma mouse cells display a protective Akt-dependent antiapoptotic pathway in response to hypoxic stimuli (Alvarez-Tejado *et al*., 2001). The protection from apoptosis by Akt could be exerted at mytocondrial level since Akt is involved in the regulation of bcl-related proteins such as Mcl-1 (Kuo *et al*., 2001). Recently, it has been reported that Akt functional inhibition by FTI can be a predictive marker of response in patients affected by cancer: this latter finding underlines the role of the inhibition of survival pathways in the determination of FTI activity. The occurrence of tumor cell resistance to FTI has been already described, based on changes in the FT expression and activity levels, or on mutational events producing insensitivity of the FT to FTI or on the activation of alternative mechanisms of prenylation of ras (i.e. geranylgeranylation) (Lebowitz and Prendergast, 1998; Sebti and Hamilton, 2000; Selleri *et al*., 2003). All these mechanisms could be responsible for the poor activity of FTI in human solid cancers even at biologically active concentrations (Smalley and Eisen, 2002).

In the present study, we have investigated if BPs can induce growth inhibition and apoptosis in epidermoid cancer cells. A 48-hour treatment with 25 μM PAM or 10 μM ZOL induced 50% growth inhibition and apoptosis in KB and H1355 cells and abolished the proliferative stimulus induced by EGF. At the same experimental conditions, a decrease of basal ras activity and an antagonism on its stimulation by EGF was recorded and the concomitant addition of farnesol to PAM-treated cells completely inhibited ras inactivation, growth inhibition and apoptosis induced by PAM. These effects were paralleled by impaired activation of the key survival enzymes Erk 1 and 2 and Akt and by their desensitization to EGF stimuli. All these latter effects were again antagonized by farnesol.

Since the concentrations of PAM and ZOL required for the antiproliferative effects *in vitro* were far from those achievable *in vivo*, we have hypothesized that BPs should be used in combination with other agents. Based on the relevance of farnesylation inhibitory effects in the BPs antitumor activity as suggested by previous findings and confirmed by our results, we have used the FTI R115777 together with PAM or ZOL and evaluated the effects of the combinatory treatment on growth inhibition and apoptosis. BPs and FTI given in combination were strongly synergistic since a CI_{50} less than 0.5 was recorded with the dedicated software Calcusyn. For instance, the DRI_{50} was of about 300-fold for PAM and FTI. Moreover, both PAM/FTI and ZOL/FTI combinations allowed the compounds to be active in terms of tumor cell growth inhibition at *in vivo* achievable therapeutic concentrations (0.1 μM range for both drugs). Finally, a potentiation of the proapoptotic effects of the two drugs was also observed in the same experimental conditions.

Notably, low concentrations of FTI induced a strong increase of ras expression with only a moderate reduction of rasAR that was, on the other hand, significantly reduced by 0.07 μM PAM. The BPs/FTI combination was able to restore the complete inactivation of ras. These data suggest that escape mechanisms to the inhibition of isoprenylation of ras might be based on the geranylgeranylation or other prenylating processes even if further studies are needed in order to find the molecular mechanisms which actually produce such effects in these cells. It could be hypothesized that BPs, inhibiting the upstream enzyme farnesylpirophosphate synthase, could prevent alternative pathways based on geranylgeranylation processes in tumor cells. However, a number of other proteins, such as the RhoB family, nuclear lamins and some tyrosin phosphatases, are also targets of farnesyl transferase (Johnston, 2001) and might be involved in the observed effects.

The impairment of ras activity induced by the combined treatment was paralleled by a reduced stimulation of both the downstream Erk and Akt survival enzymes. Again, the addition of farnesol to cells treated with the combination abolished the effects of BPs/FTI combination on apoptosis and on the activity of the signalling molecules. These data suggest that the synergistic growth inhibitory and proapoptotic effects produced by the BPs/FTI combination involve the inhibition of both Erk and Akt survival pathways acting in these cells in a ras-dependent fashion.

In conclusion, we have demonstrated that BPs induced apoptosis and growth inhibition in epidermoid cancer cells occur together with depression of ras signalling and Erk and Akt survival pathways. Moreover, BPs synergistically interacted with FTI both on antitumor activity and signalling perturbation. At our knowledge, this is the first report of a synergism between

BPs and R115777 in inducing growth inhibition and apoptosis in human cancer cells. The combination between the two inhibitors overcomes the escape mechanisms from the FTI action, which appear to be based on the activation of alternative prenylation processes, and allows the achievement of active BPs concentrations, which might be achievable *in vivo*. All these results in our opinion increase the translational potential of our *in vitro* findings and offer the basic rationale for the design of new combinatory strategies with BPs and FTIs for the treatment of tumors such as epidermoid head and neck and lung cancers, which are scarcely sensitive to conventional therapy, and can also induce symptomatic bone metastases.

Materials and methods

Materials

DMEM, BSA and FBS were purchased from Flow Laboratories (Milan, Italy). Tissue culture plasticware was from Becton Dickinson (Lincoln Park, NJ, USA). PAM was a gift of Novartis (Novartis, Basel, Switzerland). BPs were a gift of Orthobiotech (Orthobiotech, Janssen Research Center, NJ, USA). Receptor grade EGF, farnesol and protein Sepharose were purchased from Sigma (St Louis, MO, USA). Rabbit antisera raised against β-tubulin, Erk-1 K-23 and Erk-2 MAb C-14 were purchased from Santa Cruz Biotechnology (Santa Cruz, CA, USA). Rabbit antiserum raised against PARP was purchased by Upstate Biotech. (Lake Placid, NY, USA). Anti-Akt Mab and the relative activity evaluation kit were purchased by Cell Signalling. Anti-pan-Ras MAb clone 10 and U0126 were purchased from Calbiochem.

Cell culture

The human oropharyngeal epidermoid carcinoma KB and lung H1355 cancer cell lines, obtained from the American Type Tissue Culture Collection (Rockville, MD, USA), were grown in DMEM supplemented with heat-inactivated 10% FBS, 20 mM HEPES, 100 U/ml penicillin, 100 μg/ml streptomycin, 1% L-glutamine and 1% sodium pyruvate. The cells were grown in a humidified atmosphere of 95 air/5% CO_2 at 37°C.

Drug combination studies

For the study of the synergism between PAM, ZOL and R115777 on cell growth inhibition of H1355 and KB, the cells were seeded in 96-multiwell plates at the density of 5×10^3 cells/well. After 24 h incubation at 37°C, the cells were treated with different concentrations of R115777 and PAM or ZOL. Drug combination studies were based on concentration–effect curves generated as a plot of the fraction of unaffected (surviving) cells versus drug concentration (Chou and Talalay, 1984) after 72 h of treatment. To explore the relative contribution of each agent to the synergism, three combinations with different R115777/BP molar ratios were tested for each schedule: equiactive doses of the two agents (IC_{50}), higher relative doses of R115777 (IC_{75} of R115777/IC_{25} of BP) and higher relative doses of BP (IC_{25} of R115777/IC_{75} of BP). Assessment of synergy was performed quantitating drug interaction by Calcusyn computer program (Biosoft, Ferguson, MO, USA). The CI values of <1, 1 and >1 indicate synergy, additivity and antagonism, respectively (Chou *et al*., 1994).

Western blot analysis

KB cells were grown for 48 h with or without PAM or ZOL and/or EGF and/or R115777 at 37°C. For cell extract preparation, the cells were washed twice with ice-cold PBS/BSA, scraped, and centrifuged for 30 min at 4°C in 1 ml of lysis buffer (1% Triton, 0.5% sodium deoxycholate, 0.1 M NaCl, 1mM EDTA, pH 7.5, 10 mM Na_2HPO_4, pH 7.4, 10 mM PMSF, 25 mM benzamidin, 1 mM leupeptin, 0.025 U/ml aprotinin). Equal amounts of cell proteins were separated by SDS–PAGE. The proteins on the gels were electrotransferred to nitrocellulose and reacted with the different MAbs.

Affinity precipitation of Ras

KB cells were treated with PAM or ZOL and/or EGF and/or R115777 as described above. The cells were lysed in the Mg^{2+} buffer containing 20 mM HEPES, pH 7.5, 150 mM NaCl, 1% Igepal CA-630, 10 mM $MgCl_2$, 1 mM EDTA and 2% glycerol. Then, 10 μl Ras-binding domain (RBD) conjugated to agarose was added to 1 mg of cell lysate and the mixture was incubated at 4°C for 1 h. The agarose beads were collected by microcentrifugation at 14 000 *g* for 5 s and washed three times with Mg^{+2} buffer. The agarose beads were boiled for 5 min in 2 × Laemmli sample buffer and collected by a microcentrifuge pulse. The supernatants were run on 12% SDS–PAGE, then the proteins were electrotransferred on a nitrocellulose film. The nitrocellulose was incubated overnight with 1 μg/ml of anti-Ras Mab, clone RAS10 and with a secondary Mab, a goat α-mouse HRP-conjugated IgG, for 1.5 h. The film was washed with PBS/0.05% Tween 20 and detected by ECL, chemiluminescence's technique (Amersham).

Internucleosomal DNA fragmentation (Ladder)

For all apoptosis evaluation experiments (gel ladder and FACS analysis), both attached and suspended cells were collected prior the processing. DNA fragmentation was measured after extraction of low molecular weight DNA. Briefly, 10×10^6 cells were resuspended in 900 μl 1 × Tris-EDTA buffer and lysed with 25 μl 20% SDS. DNA was precipitated in ethanol for 6 h in the presence of 5 M NaCl. The high molecular weight fraction was sedimented by high-speed centrifugation, and the fragmented DNA was extracted from the aqueous phase with phenol and chloroform and then precipitated with ethanol. After resuspension in water, DNA was electrophoresed using 1.5% agarose gel and visualized by UV light following ethidium bromide staining.

Flow cytometric analysis of apoptosis

Apoptotic cell death was analysed by Annexin-V–FITC staining and by propidium iodide (PI) detection systems. Annexin-V–FITC binds to phosphatidylserine residues, which are translocated from the inner to the outer leaflet of the plasma membrane during the early stages of apoptosis. Labelling of apoptotic cells was performed using an Annexin-V kit (MedSystems Diagnostics, Vienna, Austria). Briefly, cells were incubated with Annexin-V–FITC in a binding buffer (provided by the manufacturer) for 10 min at room temperature, washed and resuspended in the same buffer as described by the manufacturer. Analysis of apoptotic cells was performed by flow cytometry (FACScan, Becton Dickinson). PI analysis of apoptosis was performed using a commercial kit (MedSystems Diagnostics, Vienna, Austria). The cells were washed in PBS, resuspended in 190 μl of prediluted binding buffer (1 : 4) and incubated for 10 min with 10 μl of the 20 mg/ml PI stock solution, and then the apoptotic cells were

analysed by FACScan flow cytometer. For each sample, 2×10^4 events were acquired. Analysis was carried out by triplicate determination on at least three separate experiments. Experiments of apoptosis induction have been also performed in the presence or absence of specific caspase inhibitors. DEVD-fmk is a specific inhibitor of caspase 3, VEID-fmk of caspase 6, DEVD-fmk of caspase 3, IETD-fmk of caspase 8, YVAD-fmk of caspase 1 and VAD-fmk is a pancaspase inhibitor (all purchased from Calbiochem, Milan, Italy).

AKT kinase assay

KB cells were treated with PAM or ZOL and/or EGF and/or R115777 as described above. At the time of processing, 1 ml ice-cold cell lysis buffer (20 mM TRIS, pH7.5, 150 mM NaCl, 1 mM EDTA, 1 mM EGTA, 1% Triton X-100, 2.5 mM sodium pyrophosphate, 1 mM β-glycerophosphate, 1 mM sodium orthovanadate, 1 μg/ml leupeptine, 1 mM PMSF) was added to cells that were incubated on ice for 10 min. The cells were collected and transferred to microcentrifuge tubes and centrifuged at 1200 *g* for 10 min at 4°C. The supernatants were collected and precipitated with 20 μl of IG1 anti-Akt monoclonal antibody immobilized with agarose beads (Cell Signaling Technology, MA, USA) by o/n incubation with gentle rocking at 4°C. The resulting immunoprecipitates were then incubated for 30 min at 30°C with 1 μg GSK-3 fusion protein (Cell Signaling Technology) in the presence of 200 μM ATP and kinase buffer (25 mM TRIS, pH 7.5, 5 mM β-glycerophosphate, 2 mM dithiotreitol, 0.1 mM sodium orthovanadate, 10 mM $MgCl_2$). The reaction was terminated with the addition of 20 μl 3 × SDS sample buffer. The supernatants were boiled for 5 min and electrophorased by 12% SDS–PAGE and the protein was electrotransferred on a nitrocellulose film. Phosphorylation of GSK-3 was detected using as probe an anti-Phospho-GSK-3α/β(Ser21/9) rabbit polyclonal antibody (diluted 1 : 1000) and then with a secondary anti-rabbit HRP-conjugated monoclonal antibody (diluted 1 : 2000). The film was washed with TBS 1 × –0.05% Tween 20 buffer and the specific reactivity was detected by chemiluminescence technique (Amersham).

Fluorescence microscopy

After washing in PBS, cells were treated with *in situ* detection kit, according to manufacturer's (SantaCruz Biotechnology, CA, USA). In details, cells were incubated with PI and an FITC-conjugated antibody raised against annexin V for at 37°C at the dark. Then, cells were observed under fluorescent microscope using a dual filter set for FITC and rhodamine. The images were acquired with a dedicated sotware.

Statistical analysis

All data are expressed as mean ± s.d. Statistical analysis was performed by analysis of variance (ANOVA) with Neumann–Keul's multiple comparison test or Kolmogorov–Smirnov where appropriate.

Acknowledgements
This work was supported by grants from Italian Minister for Research (PRIN2003) and Italian Minister of Health (FSN 2003).

References

Aikawa R, Komuro I, Yamazaki T, Zou Y, Kudoh S, Tanaka M, Shiojima I, Hiroi Y and Yazaki Y. (1997). *J. Clin. Invest.*, **100,** 1813–1821.

Ali SM, Esteva FJ, Hortobagyi G, Harvey H, Seaman J, Knight R, Costa L and Lipton A. (2001). *J. Clin. Oncol.*, **19,** 3434–3437.

Alvarez-Tejado M, Naranjo-Suarez S, Jimenez C, Carrera AC, Landazuri MO and del Peso L. (2001). *J. Biol. Chem.*, **22,** 22368–22374.

Aparicio A, Gardner A, Tu Y, Savage A, Berenson J and Lichtenstein A. (1998). *Leukemia*, **12,** 220–229.

Averbuch SD. (1993). *Cancer*, **72,** 3443–3452.

Aznar S and Lacal JC. (2001). *Cancer Lett.*, **165,** 1–10.

Benford HL, Frith JC, Auriola S, Monkkonen J and Rogers MJ. (1999). *Mol. Pharmacol.*, **56,** 131–140.

Boissier S, Ferreras M, Peyruchaud O, Magnetto S, Ebetino FH, Colombel M, Delmas P, Delaissè JM and Clézardin P. (2000). *Cancer Res.*, **60,** 2949–2954.

Cascinu S, Graziano F, Alessandroni P, Ligi M, Del Ferro E, Rossi D, Ficarelli R and Catalano G. (1998). *Support. Care Cancer*, **6,** 139–143.

Chou TC, Motzer RJ, Tong Y and Bosl GJ. (1994). *J. Natl. Cancer Inst.*, **86,** 1517–1524.

Chou TC and Talalay P. (1984). *Adv. Enzyme Regul.*, **22,** 27–55.

Coleman RE, Woll PJ, Miles M, Scrivener W and Rubens RD. (1988). *Br. J. Cancer*, **58,** 621–625.

DeSolms SJ, Ciccarone TM, MacTough SC, Shaw AW, Buser CA, Ellis-Hutchings M, Fernandes C, Hamilton KA, Huber HE, Kohl NE, Lobell RB, Robinson RG, Tsou NN, Walsh ES, Graham SL, Beese LS and Taylor JS. (2003). *J. Med. Chem.*, **46,** 2973–2984.

End DW. (1999). *Exp. New Drugs*, **17,** 241–258.

End DW, Smets G, Todd AV, Applegate TL, Fuery CJ, Angibaud P, Venet M, Sanz G, Poignet H, Kelland LR, Smith V, Valenti M, Patterson L, Clarke PA, Detre S, End D, Howes PA, Howes AJ, Dowsett M, Workman P and Johnston SRD. (2001). *Clin. Cancer Res.*, **7,** 3544–3550.

Fiordalisi JJ, Johnson II RL, Weinbaum CA, Sakabe K, Casey PJ and Cox AD. (2003). *J. Biol. Chem.*, **278,** 41718–41727.

Fleisch H. (1991). *Drugs*, **42,** 919–924.

Garrington TP and Johnson GL. (1999). *Curr. Opin. Cell. Biol.*, **11,** 211–218.

Haluska P, Dy GK and Adjei AA. (2002). *Eur. J. Cancer*, **38,** 1685–1700.

Hancock JF, Magee AI, Childs JE and Marshall CJ. (1989). *Cell*, **57,** 1167–1177.

Hilger RA, Scheulen ME and Strumberg D. (2002). *Onkologie*, **25,** 511–518.

Hughes DE, Wright KR, Uy HL, Sasaki A, Yoneda T, Roodman GD, Mundy GR and Boyce BF. (1995). *J. Bone Miner. Res.*, **10,** 1478–1487.

Johnston SR.. (2001). *Lancet Oncol.*, **2,** 18–26.

Kelland LR, Smith V, Valenti M, Patterson L, Clarke PA, Detre S, End D, Howes AJ, Dowsett M, Workman P and Johnston SRD. (2001). *Clin. Cancer Res.*, **7,** 3544–3550.

Kuo ML, Chuang SE, Lin MT and Yang SY. (2001). *Oncogene*, **20,** 677–685.

Lebowitz PF, Casey PJ, Prendergast GC and Thissen JA. (1997). *J. Biol. Chem.*, **272,** 15591–15594.

Lebowitz PF and Prendergast GC. (1998). *Oncogene*, **45,** 1439–1445.

Lee MV, Fong EM, Singer FR and Guenette RS. (2001). *Cancer Res.*, **61,** 2602–2608.
Lipton A, Glover D, Harvey H, Grabelsky S, Zelenakas K, Macerata R and Seaman J. (1994). *Ann. Oncol.*, **5,** s31–s35.
Liu B, Fang M, Lu Y, Mendelsohn J and Fan Z. (2001). *Oncogene*, **20,** 1913–1922.
Luckman SP, Hughes DE, Coxon FP, Russell RG and Rogers MJ. (1998). *J. Bone Miner. Res.*, **13,** 581–589.
Mitsui H, Takuwa N, Maruyama T, Maekawa H, Hirayama M, Sawatari T, Hashimoto N, Takuwa Y and Kimura S. (2001). *Int. J. Cancer*, **92,** 55–62.
Morton AB, Cantrill JA, Pillai GV, McMahon A, Anderson DC and Howell A. (1988). *Br. Med. J.*, **297,** 772–773.
Peng H, Wen TC, Tanaka J, Maeda N, Matsuda S, Desaki J, Sudo S, Zhang B and Sakanaka M. (1998). *J. Cereb. Blood Flow Metab.*, **18,** 349–360.
Porter AC and Vaillancourt RR. (1998). *Oncogene*, **17,** 1343–1352.
Rogers MJ, Chilton KM, Coxon FP, Lawry J, Smith MO, Suri S and Russell RG. (1996). *J. Bone Miner. Res.*, **11,** 1482–1491.
Schafer WR and Rine J. (1992). *Annu. Rev. Genet.*, **26,** 209–237.
Sebti SM and Hamilton AD. (2000). *Exp. Opin. Invest. Drugs*, **9,** 2767–2782.
Selleri C, Maciejewski JP, Montuori N, Ricci P, Visconte V, Serio B, Luciano L and Rotoli B. (2003). *Blood*, **102,** 1490–1498.
Senaratne SG, Pirianov G, Mansi JL, Arnett TR and Colston KW. (2000). *Br. J. Cancer*, **82,** 1459–1468.
Shipman CM, Rogers MJ, Apperley JF, Russell RG and Croucher PI. (1997). *Br. J. Haematol.*, **98,** 665–672.
Sibilia M, Fleischmann A, Behrens A, Stingl L, Carroll J, Watt FM, Schlessinger J and Wagner EF. (2000). *Cell*, **102,** 211–220.
Smalley KSM and Eisen TG. (2002). *Int. J. Cancer*, **98,** 514–518.
Stoll SW, Benedict M, Mitra R, Hiniker A, Elder JT and Nunez G. (1998). *Oncogene*, **16,** 1493–1499.
Tamanoi F, Kato-Stankiewicz J, Jiang C, Machado I and Thapar N J.. (2001). *Cell. Biochem.*, **37,** 64–70.
Tassone P, Forciniti S, Galea E, Morrone G, Turco MC, Martinelli V, Tagliaferri P and Venuta S.. (2000). *Leukemia*, **14,** 841–844.
Tassone P, Tagliaferri P, Viscomi C, Palmieri C, Caraglia M, D'Alessandro A, Galea E, Goel A, Abbruzzese A, Boland CR and Venuta S. (2003). *Br. J. Cancer*, **88,** 1971–1978.
Tilly JL, Billig H, Kowalski KI and Hsueh AJ. (1992). *Mol. Endocrinol.*, **6,** 1942–1950.
Twiss IM, Pas O, Ramp-Koopmanschap W, Den Hartigh J and Vermeij P. (1999). *J. Bone Miner. Res.*, **14,** 784–791.
Van Beek E, Pieterman E, Cohen L, Lowik C and Papapoulos C. (1999a). *Biochem. Biophys. Res. Commun.*, **255,** 491–494.
Van Beek E, Pieterman E, Cohen L, Lowik C and Papapoulos S. (1999b). *Biochem. Biophys. Res. Commun.*, **264,** 108–111.
Vitale G, Fonderico F, Martignetti A, Caraglia M, Ciccarelli A, Nuzzo V, Abbruzzese A and Lupoli G. (2001). *Br. J. Cancer*, **84,** 1586–1590.
von Gise A, Lorenz P, Wellbrock C, Hemmings B, Berberich-Siebelt F, Rapp UR and Troppmair. (2001). *J. Mol. Cell. Biol.*, **21,** 2324–2336.
Widmann C, Gibson S, Jarpe MB and Johnson GL. (1999). *Physiol. Rev.*, **79,** 143–180.
Wood J, Bonjean K, Ruetz S, Bellahcène A, Devy L, Foidart JM, Castronovo V and Green JR. (2002). *J. Pharm. Exp. Therap.*, **302,** 1055–1061.
Yan CYI and Greene LA. (1998). *J. Neurosci.*, **18,** 4042–4049.
Zhou H, Li X-M, Meinkoth J and Pittman RN. (2000). *J. Cell Biol.*, **151,** 483–494.